

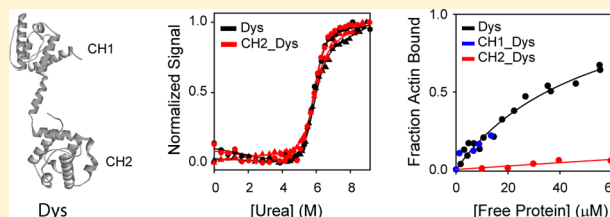
# The N- and C-Terminal Domains Differentially Contribute to the Structure and Function of Dystrophin and Utrophin Tandem Calponin-Homology Domains

Surinder M. Singh,<sup>†</sup> Swati Bandi,<sup>†</sup> and Krishna M. G. Mallela<sup>\*,†,‡</sup>

<sup>†</sup>Department of Pharmaceutical Sciences, Skaggs School of Pharmacy and Pharmaceutical Sciences, and <sup>‡</sup>Program in Structural Biology and Biochemistry, University of Colorado Anschutz Medical Campus, Aurora, Colorado 80045, United States

## S Supporting Information

**ABSTRACT:** Dystrophin and utrophin are two muscle proteins involved in Duchenne/Becker muscular dystrophy. Both proteins use tandem calponin-homology (CH) domains to bind to F-actin. We probed the role of N-terminal CH1 and C-terminal CH2 domains in the structure and function of dystrophin tandem CH domain and compared with our earlier results on utrophin to understand the unifying principles of how tandem CH domains work. Actin cosedimentation assays indicate that the isolated CH2 domain of dystrophin weakly binds to F-actin compared to the full-length tandem CH domain. In contrast, the isolated CH1 domain binds to F-actin with an affinity similar to that of the full-length tandem CH domain. Thus, the obvious question is why the dystrophin tandem CH domain requires CH2, when its actin binding is determined primarily by CH1. To answer, we probed the structural stabilities of CH domains. The isolated CH1 domain is very unstable and is prone to serious aggregation. The isolated CH2 domain is very stable, similar to the full-length tandem CH domain. These results indicate that the main role of CH2 is to stabilize the tandem CH domain structure. These conclusions from dystrophin agree with our earlier results on utrophin, indicating that this phenomenon of differential contribution of CH domains to the structure and function of tandem CH domains may be quite general. The N-terminal CH1 domains primarily determine the actin binding function whereas the C-terminal CH2 domains primarily determine the structural stability of tandem CH domains, and the extent of stabilization depends on the strength of inter-CH domain interactions.



Actin is a vital component of the cytoskeleton necessary for maintaining the structural integrity and homeostasis of eukaryotic cells.<sup>1</sup> Actin-binding proteins play major roles in the structural dynamism of the actin cytoskeleton, thus controlling various biological functions that include muscle physiology. These proteins use well-defined structural domains to bind to actin. Of all known actin-binding domains (ABDs), tandem calponin-homology (CH) domains are the most common and most widespread.<sup>2–4</sup> These ABDs consist of two CH domains (N-terminal CH1 and C-terminal CH2) in tandem (Figure 1). Each CH domain typically consists of ~120 residues with characteristic globular calponin-like structure made up of four major helices forming the core of the domain, and two or three minor helices interconnected by loops of variable lengths making a minor structural contribution. Despite their widespread occurrence, structural determinants of their actin binding are poorly understood. In this work, we present our results on the tandem CH domain of dystrophin and compare them with our earlier results on the utrophin tandem CH domain to deduce the unifying principles underlying how tandem CH domains work.

Studying the tandem CH domains of dystrophin and utrophin is particularly important in understanding the disease mechanisms of muscular dystrophy. Genetic mutations in dystrophin trigger Duchenne/Becker muscular dystrophy.<sup>5</sup> The

main function of dystrophin is to maintain the structural integrity of the muscle cells during muscle contraction and stretch. Dystrophin connects cytoskeletal filamentous actin (F-actin) to the sarcolemmal glycoprotein complex.<sup>6,7</sup> Utrophin is its closest homologue and is being explored to replace the loss of functional dystrophin in human patients.<sup>8,9</sup> Both proteins use their tandem CH domains for binding to actin.<sup>6,7</sup> Therefore, studying the structure–function relationship of tandem CH domains will lead to a better understanding of the biological role of these two proteins. In addition, a major fraction of disease-causing missense mutations in dystrophin occur in its tandem CH domain.<sup>5,10,11</sup> Miniaturized versions of dystrophin and utrophin, known as mini- and microproteins, are being explored in gene therapy trials to replace the loss of functional dystrophin.<sup>8,9</sup> However, these shortened proteins have decreased stability and functionality.<sup>12–14</sup> All these proteins contain in common tandem CH domains. Hence, studying the physical principles underlying the structure and function of tandem CH domains may lead to improved gene and protein constructs for treating muscular dystrophy patients.

Received: September 1, 2015

Revised: October 29, 2015

Published: October 30, 2015

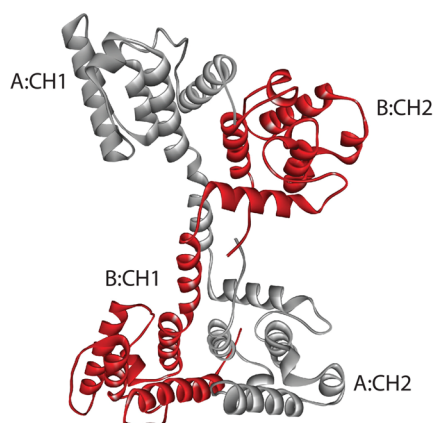


**Figure 1.** X-ray crystal structure of the dystrophin tandem CH domain (Protein Data Bank entry 1DXX). The protein crystallizes as an antiparallel domain-swapped dimer,<sup>18</sup> although it exists as a monomer in solution.<sup>10,30,46,48</sup> The two monomers labeled A and B in the dimeric crystal structure are colored gray and red, respectively.

The quest for identifying the structural determinants of actin binding of dystrophin and utrophin tandem CH domains began 25 years ago.<sup>15</sup> Initial peptide binding experiments proposed three actin-binding surfaces (ABSs).<sup>16,17</sup> However, subsequently determined X-ray structures showed that these regions are oriented in opposite directions,<sup>18,19</sup> thus leading to questions about whether all three regions are equally important in actin binding. In the tandem CH domains of dystrophin and utrophin, the N-terminal CH1 domains contain ABS1 and ABS2 whereas the C-terminal CH2 domains contain ABS3. Experiments on truncated proteins qualitatively indicated that part of CH1 containing ABS1 binds to F-actin without ABS2 or ABS3.<sup>15,20</sup> Another truncated construct containing part of ABS2 in the CH1 and CH2 domain binds to F-actin, but with decreased affinity compared to that of the full-length tandem CH domain.<sup>20</sup> However, these truncated proteins used solubility tags, such as maltose-binding proteins, much larger than the constructs themselves,<sup>15</sup> which may force the CH domains into non-native structures. Hence, these earlier data on truncated proteins remained ambiguous.

We have previously examined the actin binding function of individual CH domains in utrophin with respect to its full-length tandem CH domain.<sup>21</sup> Our results indicate that the actin binding is primarily determined by the N-terminal CH1 domain. In the second study,<sup>22</sup> we compared the structural stability of the isolated C-terminal CH2 domain with that of the full-length utrophin tandem CH domain. The utrophin CH2 domain appears to be as stable as that of the full-length tandem CH domain. These two results, when analyzed together, suggest the differential role played by the two CH domains; in particular, CH1 controls actin binding function, whereas CH2 controls structural stability. This hypothesis, never stated in the literature, contradicts the conventional thinking that cooperativity between the two CH domains determines the actin binding. We rather showed that the role of CH2 is just to stabilize the tandem domain structure, and not in controlling actin binding. This hypothesis seems to be controversial, and hence, it is important to show whether these conclusions hold good in other tandem CH domains or whether it is just a coincidental property of the utrophin tandem CH domain. In this work, we analyze the actin binding and structural stability of isolated CH domains of dystrophin.

## ■ MATERIALS AND METHODS

**Cloning, Expression, and Purification of the Full-Length Dystrophin Tandem CH Domain and Its Isolated CH Domains.** The plasmid vector for the dystrophin tandem CH domain (residues 1–246) was cloned using the coding DNA into the pET28a plasmid using NdeI and HindIII restriction endonuclease sites. Ligation mix was transformed into DH5 $\alpha$  by heat shock. The plasmid was amplified using the Qiagen miniprep kit, and the construct was confirmed by DNA sequencing. Constructs for the CH1 domain (residues 1–130) were created by introducing a stop codon using quick mutagenesis (Qiagen). The cDNA corresponding to the CH2 domain (residues 131–246) was amplified from that of the full-length tandem CH domain using polymerase chain reaction and subcloned into the pET-SUMO expression vector using BamHI and XhoI restriction endonuclease sites. Constructs were confirmed by DNA sequencing and transformed into BL21(DE3). Proteins were expressed and purified using Ni-His affinity chromatography. When CH2 was expressed in the pET-SUMO vector, the N-terminal SUMO fragment was cleaved using Ulp1 protease,<sup>23</sup> and pure protein was isolated in the flow-through using a Ni-His affinity column. The full-length dystrophin tandem CH domain and its isolated CH2 domain were expressed as soluble proteins and hence were purified in their native state. On the other hand, the CH1 domain was expressed in inclusion bodies and purified in its denatured state in 8 M urea.

**Circular Dichroism (CD).** The full-length dystrophin tandem CH domain and its isolated CH2 domain (1  $\mu$ M proteins) in phosphate-buffered saline (PBS) [100 mM NaH<sub>2</sub>PO<sub>4</sub> and 150 mM NaCl (pH 7)] were used for measuring CD (Chirascan Plus, Applied Photophysics). The mean residue ellipticity (MRE) of the protein was calculated from the CD values in millidegrees.<sup>24</sup>

**Thermal Melts.** For the full-length dystrophin tandem CH domain and its isolated CH2 domain (1  $\mu$ M each in PBS), changes in the far-UV CD signal at 222 nm were monitored as a function of increasing solution temperature at a temperature ramp of 1  $^{\circ}$ C/min (Chirascan Plus, Applied Photophysics). For fluorescence thermal melts, the samples were excited at 280 nm and the emission at 360 nm was monitored as a function of increasing temperature at a temperature ramp of 1  $^{\circ}$ C/min (PTI QuantaMaster fluorometer). Thermal melts were fit to a sigmoidal equation with sloped native and unfolded baselines to determine the midpoint melting temperature,  $T_m$ .

**Differential Scanning Calorimetry (DSC).** DSC thermograms were recorded at a protein concentration of 20  $\mu$ M in PBS with a thermal scan rate of 90  $^{\circ}$ C/h (VP-DSC, MicroCal, Malvern, PA). Over the temperature range we used, PBS buffer does not change its pH<sup>25,26</sup> and is recommended as one of the best buffers for DSC by the instrument vendors. The peak maximum in the denaturation endotherm was used as the  $T_m$ .

**Refolding Yields.** Refolding yields were determined by diluting the denatured proteins in 8 M urea (10  $\mu$ M protein stocks) 10 times into PBS buffer. Samples were then centrifuged at  $\sim$ 30000g, and supernatants were subjected to protein quantification using the absorbance. Molecular extinction coefficients for all variants were calculated from their amino acid sequence using PROTPARAM software at ExPASy (<http://www.expasy.org/>).

**Denaturant Melts.** For urea denaturation melts of the full-length dystrophin tandem CH domain and its isolated CH2

domain, 1  $\mu\text{M}$  protein in PBS buffer was used. Changes in the far-UV CD signal at 222 nm and intrinsic protein fluorescence of aromatic amino acids (excitation at 280 nm, emission at 360 nm) were monitored as a function of the increasing urea concentration. Denaturant melts were fit to a two-state equilibrium unfolding model using Santoro–Bolen linear extrapolation equations<sup>27,28</sup> to determine the Gibbs free energy of unfolding,  $\Delta G_{\text{unf}}$ .

**Actin Binding Affinity of the Full-Length Dystrophin Tandem CH Domain and Its CH2 Domain.** Skeletal muscle G-actin (Cytoskeleton, Denver, CO) was polymerized (7  $\mu\text{M}$ ) and incubated with varying concentrations of the binding partner protein (either tandem CH domain or isolated CH2) for 5 min at room temperature. This mixture (final volume of 100  $\mu\text{L}$ ) was centrifuged at 100000g for 30 min (sw55Ti rotor, Beckman Optima LE80K), and pellets were solubilized in 30  $\mu\text{L}$  of sodium dodecyl sulfate–polyacrylamide gel electrophoresis (SDS–PAGE) loading buffer. Half of this was boiled and subjected to SDS–PAGE and stained with Coomassie blue. The intensity of the individual bands was determined using Quantity One on a Bio-Rad Gel Doc XR instrument. Intensity values for actin bands were corrected by multiplying with the correction factors obtained from the BSA standard curve to account for the differential staining of the dye to proteins.<sup>21,29,30</sup> The ratio of the band intensities was used to determine the fraction of F-actin bound using the following formula: fraction actin bound = (corrected band intensity of bound protein  $\times$  molecular weight of actin)/(corrected band intensity of actin  $\times$  molecular weight of bound protein). The free protein concentration was calculated using the following formula: free protein = total protein added – (fraction actin bound  $\times$  concentration of total actin added). The binding data were fit to the equation

$$\text{fraction actin bound} = B_{\text{max}}x/(K_d + x) \quad (1)$$

where  $x$  is the free protein concentration,  $B_{\text{max}}$  is the maximal number of binding sites, and  $K_d$  is the dissociation constant.<sup>30</sup>

**Actin Binding Affinity of the CH1 Domain.** The isolated CH1 domain purified in its denatured state could not be refolded. Hence, its actin binding was measured by refolding the protein by diluting the denaturant 20 times starting from its denatured state (8 M urea) in the presence of F-actin.<sup>21</sup> Insoluble aggregates of free CH1 were removed using low-speed centrifugation (10000g for 8 min). Supernatants were treated essentially the same as described above for the CH2 domain.

## RESULTS

**Biophysical Characterization of the Full-Length Dystrophin Tandem CH Domain and Its Isolated CH Domains.** The dystrophin tandem CH domain and its isolated CH domains were purified to homogeneity (Figure 2A). Band positions on 12% SDS–PAGE match with the expected molecular weights of the purified monomeric proteins. Full-length tandem CH domains and its CH2 domain were expressed as soluble proteins, whereas CH1 was expressed in inclusion bodies. The CH1 domain was purified in its denatured state. It could not be refolded back by diluting the denaturant. Most of the CH1 resulted in protein aggregates.

The dystrophin tandem CH domain and its isolated CH2 domain were subjected to biophysical characterization. Figure 2B shows the CD spectra of the dystrophin tandem CH domain and its isolated CH2 domain. Negative peaks at 208

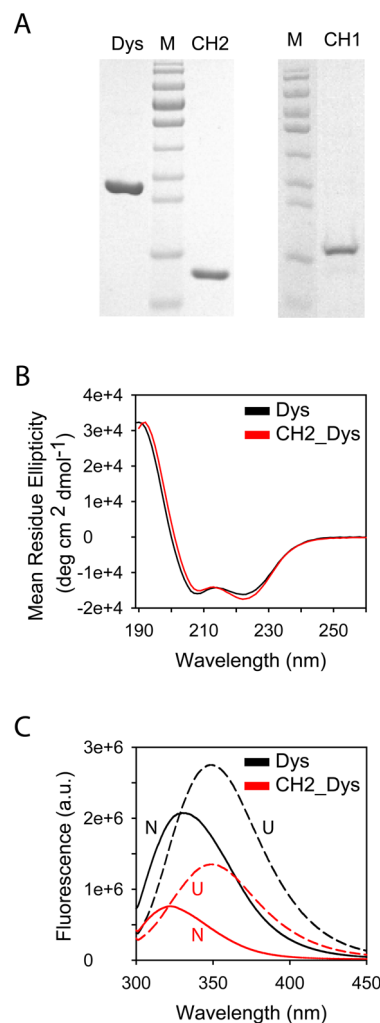


**Figure 2.** (A) SDS–PAGE of the purified dystrophin tandem CH domain and its CH domains. Lane M contained the molecular mass markers (from bottom to top, 10, 15, 25, 35, 40, 55, 70, 100, 130, and 170 kDa, respectively). (B) Circular dichroism (CD) spectra of the dystrophin tandem CH domain (black) and its CH2 domain (red). (C) Fluorescence spectra of the native (N) and unfolded (U) states of the dystrophin tandem CH domain (black) and its CH2 domain (red).

and 222 nm are characteristic of an  $\alpha$ -helical secondary structure.<sup>24</sup> Well-defined CD spectra with such minima for the dystrophin tandem CH domain and its isolated CH2 domain indicate that both are well-folded,  $\alpha$ -helical proteins. This observation is consistent with the  $\alpha$ -helical crystal structure of the dystrophin tandem CH domain (Figure 1). We also used the intrinsic protein fluorescence of aromatic amino acids to determine the well-folded nature of the dystrophin tandem CH domain and its CH2 domain. Figure 2C shows the fluorescence spectra of native (N) and unfolded (U) states of the two proteins. The dystrophin tandem CH domain has eight tryptophans and five tyrosines. These aromatic residues are well-dispersed across the protein structure. Because fluorescence originates from the aromatic side chains, it can be used as a probe for the tertiary structure of proteins. The emission maximum for the native tandem CH domain (330 nm) was shifted to longer wavelengths after denaturation (348 nm). A similar postdenaturation red shift in the emission maxima was also observed for the isolated CH2 domain. They were 322 nm for native CH2 and 349 nm for denatured CH2. A red shift in

fluorescence upon denaturation indicates the buried nature of tryptophan residues in native proteins and is a hallmark of well-folded proteins.<sup>31</sup>

### Thermodynamic Stability of the Full-Length Dystrophin Tandem CH Domain and Its Isolated CH2 Domain.

Thermal denaturation and chemical denaturation are two commonly used methods for characterizing protein stability.<sup>32,33</sup> In thermal melts, the solution temperature was increased at a constant rate, and the changes in protein signals were measured. Panels A and B of Figure 3 show the thermal

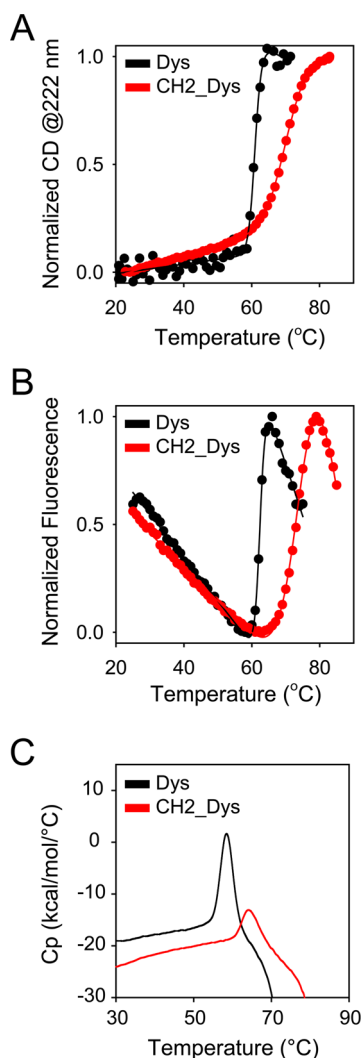


**Figure 3.** Structural stability of the dystrophin tandem CH domain and its CH2 domain probed using temperature melts and differential scanning calorimetry (DSC). (A) Changes in the CD signal at 222 nm of the tandem CH domain (black) and its CH2 domain (red) as a function of increasing solution temperature. (B) Changes in the intrinsic protein fluorescence of the tandem CH domain (black) and its CH2 domain (red) as a function of increasing solution temperature. (C) DSC thermograms for the tandem CH domain (black) and its CH2 domain (red).

melts for the dystrophin tandem CH domain and its CH2 domain. For both, thermally denatured proteins could not be renatured by decreasing the temperature as most proteins resulted in aggregates. Because of the irreversibility of thermal melts, they are more qualitative in nature as determined by comparison of the relative stabilities of the dystrophin tandem

CH domain and its isolated CH2 domain. When protein unfolding was monitored as a function of an increasing solution temperature using the CD signal at 222 nm as a probe for the  $\alpha$ -helical secondary structure (Figure 3A), the CH2 domain required higher temperature to unfold compared to the tandem CH domain. The midpoint melting temperature ( $T_m$ ) values were determined by fitting the thermal melts to a sigmoidal function with sloped pre- and post-transition baselines. The  $T_m$  value for the CH2 domain ( $71.0 \pm 0.2$  °C) was significantly higher than that of the full-length tandem CH domain ( $61.0 \pm 0.1$  °C). A similar trend was observed when the thermal melts were monitored using intrinsic protein fluorescence as a probe for the tertiary structure of proteins (Figure 3B). The CH2 domain melted at higher temperature than the full-length tandem CH domain. The  $T_m$  value for the CH2 domain was  $75.9 \pm 0.4$  °C, which was significantly higher than that of the full-length tandem CH domain ( $62.4 \pm 0.1$  °C). These thermal melts monitored using two optical probes, CD and fluorescence, suggest that the isolated CH2 domain is highly stable compared to the full-length tandem CH domain. A possible explanation of why the  $T_m$  values for CH2 are higher than those for the full-length protein is that the aggregation of tandem CH domain may be determined by CH1 unfolding. Similar to that observed in the utrophin tandem CH domain,<sup>32</sup> the first domain that is unfolding with temperature may be the CH1 domain in the dystrophin tandem CH domain. Because CH1 has stronger aggregation propensity than that of CH2 (Figure 4A), we may not observe the thermal unfolding of CH2

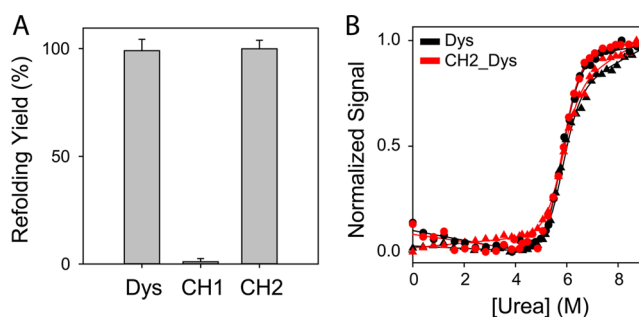


**Figure 4.** Refolding yields and structural stabilities of the dystrophin tandem CH domain and its CH2 domain probed using denaturant melts. (A) Refolding yields of the dystrophin tandem CH domain and its CH domains starting from their unfolded states in 8 M urea. Both the tandem CH domain and the CH2 domain fold reversibly, whereas the CH1 domain aggregates severely. (B) Changes in the CD signal at 222 nm (circles) and in the intrinsic protein fluorescence (triangles) of the tandem CH domain (black) and its CH2 domain (red) as a function of increasing urea concentration.

because of protein aggregation induced by CH1 unfolding. Note that the  $T_m$  values determined by fluorescence slightly differ from those determined by CD, possibly because CD measures the melting of secondary structure, whereas the fluorescence measures the melting of the tertiary structure of proteins.

The thermal stability of proteins was also monitored independently by differential scanning calorimetry (DSC). This technique measures the amount of additional heat required to increase the temperature of the protein sample with respect to the buffer reference, rather than measuring changes in optical signals as in the methods described above. Figure 3C shows the endothermic unfolding DSC curves for

the dystrophin tandem CH domain and its CH2 domain. The DSC curves shown are the raw data as obtained directly from the instrument for the protein samples with respect to the buffer reference without applying any corrections to account for sloped baselines. Consistent with the thermal melts measured by optical signals (Figure 3A,B), the CH2 domain melted at a higher temperature than the full-length tandem CH domain. The  $T_m$  values in DSC endotherm corresponding to the peak maximum heat change were  $64.2 \pm 0.2$  °C for the isolated CH2 domain and  $58.5 \pm 0.1$  °C for the full-length tandem CH domain. These  $T_m$  values again indicate that the CH2 domain has a higher thermal stability than that of the full-length tandem CH domain. In these DSC curves, a clear unfolded baseline was not observed because of exothermic protein aggregation occurring immediately after protein unfolding, as indicated by a drastic decrease in heat capacity at higher temperatures. Hence, these data could not be analyzed to determine equilibrium thermodynamic parameters. Note that the  $T_m$  values determined by DSC are skewed toward lower temperatures compared to those determined by optical spectroscopies (Figure 3A,B), because of the near-simultaneous protein aggregation in the DSC experiment while the protein is unfolding.

The thermal denaturation data given above for the dystrophin CH domain are quite consistent with our earlier results on utrophin CH domains<sup>22</sup> (also shown in Figure S1A,B). Similar to dystrophin, utrophin CH2 unfolds at higher temperatures, indicating its higher stability than that of the utrophin tandem CH domain.

To probe the true equilibrium thermodynamic stability, we monitored the protein unfolding with the addition of urea using changes in protein CD and fluorescence signals. Because the reversibility of folding is a prerequisite for determining thermodynamic parameters, it was confirmed by subjecting the proteins to refolding yield experiments (Figure 4A). Both the dystrophin tandem CH domain and its CH2 domain were denatured in 8 M urea and refolded back into native forms by diluting the denaturant 10 times. Both refolded by ~100%, indicating that their urea unfolding is completely reversible. As mentioned before, the CH1 domain could not be refolded starting from its unfolded state (Figure 4A), and resulted in protein aggregates.

We further confirmed that the inability of CH1 to refold is not due to any covalent modifications that may occur because of the high urea concentration (8 M) used to unfold proteins (Figure S2). Urea degrades with time into ammonium cyanate.<sup>32</sup> High concentrations of cyanate, in the range of hundreds of millimoles, can result in the chemical modification of proteins.<sup>34</sup> Such urea degradation occurs at elevated temperatures (>90 °C) and at extreme pH values but is very slow at room temperature and at neutral pH values.<sup>35</sup> Urea degradation also depends on the solution impurities and can be drastically slowed by using highly pure urea.<sup>32,36</sup> We used matrix-assisted laser desorption ionization time-of-flight (MALDI-TOF) mass spectrometry (MS) to show the absence of protein covalent modifications, and Fourier transform infrared (FT-IR) spectroscopy to show the absence of urea degradation under our experimental conditions (Figure S2). MS indicated identical protein molecular mass in the absence and presence of 8 M urea (Figure S2A). FT-IR showed no evidence of cyanate, as indicated by the absence of a characteristic vibrational frequency at  $\sim 2200$   $\text{cm}^{-1}$ <sup>37,38,49</sup> (Figure S2B).

To determine equilibrium stability, denaturation melts were monitored using the CD signal at 222 nm as a probe for the secondary structure and the intrinsic protein fluorescence as a probe for the tertiary structure of proteins (Figure 4B). The urea denaturation curves for CH2 are very similar to that of the tandem CH domain. Consistently, all four denaturant curves could be globally fitted to a Santoro–Bolen two-state equilibrium unfolding model<sup>27,28</sup> to obtain the Gibbs free energy of unfolding ( $\Delta G_{\text{unf}} = 9.98 \pm 0.33$  kcal/mol). These denaturant melts, along with the inability of CH1 to refold (Figure 4A), indicate that the structural stability of dystrophin tandem CH domain predominantly originates from its CH2 domain. These equilibrium stability results for dystrophin CH domains were consistent with our earlier results on utrophin CH domains<sup>22</sup> (Figure S1C), where we have shown that the stability of the utrophin tandem CH domain is primarily determined by its CH2 domain.

Because tandem CH domains consist of two structural domains, a more appropriate way of obtaining their true  $\Delta G_{\text{unf}}$  is by fitting their denaturant melts to a three-state model with the existence of an intermediate.<sup>39</sup> However, we could not fit the data shown in Figure 4B or Figure S1C to a three-state model with a unique set of fitting parameters, because of the absence of a clear double-sigmoidal transition. Hence, the reported  $\Delta G_{\text{unf}}$  value for the tandem CH domains represent the apparent or the signal-weighted, ensemble-averaged stabilities.

The refolding experiments on the dystrophin CH domains described above (Figure 4A) and similar results for utrophin CH domains<sup>21,22</sup> indicate that CH2 acts like a molecular chaperone to aid refolding of CH1. To obtain further evidence that CH1 is in fact unstable in the absence of CH2, we probed the structure and stability of refolded utrophin CH1. Although ~99% of the protein aggregated, we could recover ~1% as a soluble protein. This utrophin CH1 without CH2 is predominantly of random-coil structure (Figure S3A) and shows incomplete thermal and denaturant melts with missing native baselines (Figure S3B,C), when compared to those of the full-length utrophin tandem CH domain (Figure S1C). These structure and stability comparisons indicate that the presence of CH2 stabilizes CH1. A similar characterization could not be performed on dystrophin CH1, because we could not obtain sufficient quantities of refolded protein, indicating its stronger tendency to aggregate compared to the utrophin CH1.

**Actin Binding of the Dystrophin Tandem CH Domain and Its Isolated CH Domains.** The purified, soluble dystrophin tandem CH domain and its isolated CH2 domain were subjected to high-speed actin cosedimentation assays.<sup>21,40,41</sup> A fixed concentration of F-actin (7  $\mu\text{M}$ ) was titrated with varying concentrations (0–60  $\mu\text{M}$ ) of the indicated protein. The solutions were subjected to high-speed cosedimentation, and the pellets were loaded onto a SDS–PAGE gel (Figure 5A,B). Using densitometry and after correction for the differential staining of the dye to proteins,<sup>21,29,30</sup> the fraction of actin bound to each protein was calculated and plotted versus the concentration of free actin-binding partners.

Using a method we have previously developed for measuring actin binding of the unstable utrophin CH1 domain,<sup>21</sup> actin binding of the dystrophin CH1 domain was measured by refolding the protein starting from its unfolded state in the presence of F-actin. This resulted in a competition between actin binding and aggregation. Aggregates were pelleted by low-speed centrifugation, followed by high-speed centrifugation of

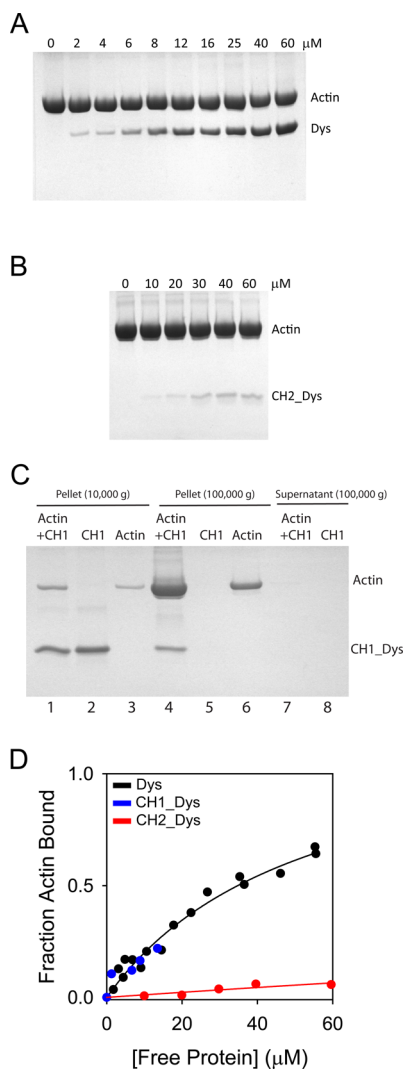


**Figure 5.** Actin binding of the dystrophin tandem CH domain and its CH domains. (A and B) Actin binding cosedimentation assays of the tandem CH domain and its CH2 domain. Shown are SDS–PAGE gels of the pellets from high-speed centrifugation performed at a fixed concentration of F-actin (7  $\mu\text{M}$ ) and with varying concentrations of the binding protein. (C) Actin binding of the CH1 domain at one particular CH1 concentration (5  $\mu\text{M}$ ). Denatured CH1 was refolded from its unfolded state in the presence of F-actin. As a control, the unfolded CH1 domain was refolded in the absence of F-actin. F-Actin alone without CH1 was used as the second control. The three samples were initially subjected to low-speed centrifugation to pellet the CH1 aggregates. The supernatants were then subjected to high-speed centrifugation, and SDS–PAGE of the pellets was used to quantify the fraction of actin bound. Shown is a SDS–PAGE gel of the pellets when the sample and the two controls were subjected to low-speed centrifugation (10000g) (lanes 1–3), the pellets when the supernatants of low-speed centrifugation were subjected to high-speed centrifugation (100000g) (lanes 4–6), and the supernatants after high-speed centrifugation (lanes 7 and 8). All the CH1 aggregates were pelleted during the low-speed centrifugation step, as indicated by lanes 2 and 5. We have previously shown that the residual urea present in the sample (0.4 M) after diluting the denatured CH1 20 times does not depolymerize F-actin.<sup>21</sup> (D) Actin binding curves of the dystrophin tandem CH domain (black), CH1 (blue), and CH2 (red).

the supernatants resulted in pelleting F-actin and bound proteins. The pellets were loaded onto a SDS–PAGE gel. Figure 5C shows the result at one particular CH1 concentration

(5  $\mu\text{M}$ ). As before, densitometry was used to quantitate the individual bands, from which the fraction actin bound was calculated.

Actin binding curves of the dystrophin tandem CH domain and its isolated CH domains are shown in Figure 5D. The data were fit to the binding equation (eq 1 in Materials and Methods) to determine the dissociation constants ( $K_d$ ). The full-length dystrophin tandem CH domain binds to F-actin with a  $K_d$  of  $47.05 \pm 13.92 \mu\text{M}$  and a  $B_{\text{max}}$  of  $1.17 \pm 0.16$  ( $P$  value  $< 0.0001$ ). In comparison, the CH2 domain did not show significant actin binding. If the  $B_{\text{max}}$  value was set to 1, actin binding data of CH2 could be fit with a  $K_d$  of  $863 \pm 102 \mu\text{M}$  ( $P = 0.0004$ ). Although a full binding curve for the CH1 domain could not be obtained, the rising edge of the curve appears as if it is binding to F-actin with an affinity nearly equal to that of the full-length dystrophin tandem CH domain. Further evidence for the predominant contribution of CH1 to the actin binding affinity of the tandem CH domain comes from our recently published work.<sup>42</sup> Tandem CH domains are made up of three structural elements that can determine actin binding: the two CH domains (CH1 and CH2) and the inter-CH domain linker. Because isolated CH2 does not significantly bind to actin compared to the full-length tandem CH domain (Figure 5D), the major contribution to actin binding has to be either from the intrinsic actin binding affinity of the CH1 domain or from the inter-CH domain interactions modulated by the interdomain linker. We have recently shown that the interdomain linker does not significantly affect the actin binding of tandem CH domains.<sup>42</sup> Therefore, the actin binding affinity of the full-length dystrophin tandem CH domain has to be from the CH1 domain, consistent with the conclusions drawn from Figure 5D. This is also in agreement with our earlier actin binding results on the utrophin tandem CH domain<sup>21</sup> (data shown in Figure S4), where we showed that the actin binding affinity is predominantly determined by the CH1 domain.

■ DISCUSSION

**Differential Contribution of Individual CH Domains Might Be a General Phenomenon in the Family of Tandem CH Domains.** Despite tandem CH domains being the most common and most widespread actin-binding domains in proteins,<sup>2–4</sup> structural determinants of their function are less understood. Results presented here and in our earlier studies<sup>21,22</sup> provide quantitative insight into the role of individual CH domains in the structure and function of dystrophin and utrophin tandem CH domains. The N-terminal CH1 domains control the actin binding function, whereas the C-terminal CH2 domains control the structural stability. Although scarce, functional data on one other tandem CH domain support this conclusion. The only published quantitative data are from  $\alpha$ -actinin.<sup>40</sup> The full-length tandem CH domain, isolated CH1, and isolated CH2 of  $\alpha$ -actinin bind to F-actin with  $K_d$  values of 4.3, 57, and  $>1000 \mu\text{M}$ , respectively.<sup>40</sup> This order matches our results for dystrophin and utrophin CH domains. Consistently, recent phylogenetic analysis suggests that the N-terminal CH1 domain is primarily responsible for the interaction of dystrophin with the actin cytoskeleton.<sup>43</sup> No experimental studies on the stability of individual CH domains in any tandem CH domain have been performed to date, except our earlier work on utrophin.<sup>22</sup> Indirect evidence of the differential contribution of CH domains to the structural stability comes from the literature. Molecular structures have been determined for isolated CH2



determine their actin binding, whereas the C-terminal CH2 domains determine their structural stability. These differences in the relative contribution of CH domains may originate from their differences in the primary structures and how these differences are manifested in their tertiary structures (Figure 6). The CH1 domains of dystrophin and utrophin are 88% similar in amino acid sequence.<sup>48</sup> Similarly, CH2 domains of dystrophin and utrophin are 85% similar in sequence.<sup>48</sup> However, when a CH1 domain is compared with the respective CH2 domain from the same protein, they are only 40% similar in the case of dystrophin and 31% similar in the case of utrophin (Figure 6A,B). These sequential differences lead to differences in their tertiary structures. Although the CH1 domains of dystrophin and utrophin are structurally similar, and respectively their CH2 domains,<sup>48</sup> clear tertiary structural differences exist between the CH1 and CH2 domains from the same protein (Figure 6C,D). Regular secondary structures such as  $\alpha$ -helices occur at identical positions, but dystrophin CH2 differs from its CH1 domain in terms of the loop structures (Figure 6C). Similar differences in loop structures also exist between the CH1 and CH2 domains of utrophin (Figure 6D). In addition, the loop regions in CH2 domains are more structured than the loop regions in CH1 domains, implying that the higher structural stability of CH2 may originate from the nature of their interhelical loops. These comparisons suggest that the differential contribution of CH domains may be built into their primary and tertiary structures. Furthermore, it is interesting to note that although CH2 does not seem to determine actin binding when compared to CH1, the location of ABS3 in the CH2 domains is at identical positions in both primary and tertiary structures as that of ABS1 in the CH1 domains (Figure 6). This indicates that both CH domains might have evolved from the same ancestor<sup>2,43</sup> but have diverged because of the necessity of stabilizing the protein structure while performing function, thus leading to differences in their relative contributions to the structure and function of tandem CH domains. It is very rare to find tandem domain proteins with two identical domains performing different functions and shows how nature has beautifully evolved the tandem CH domain structures to optimize their actin binding function and structural stability by varying the loop regions connecting the regular secondary structural elements.

## ■ ASSOCIATED CONTENT

### ■ Supporting Information

The Supporting Information is available free of charge on the ACS Publications website at DOI: 10.1021/acs.biochem.5b00969.

Structural stability of the utrophin tandem CH domain and its isolated CH2 domain (Figure S1), characterization of protein covalent modifications and urea degradation (Figure S2), structure and stability of isolated CH1 of utrophin (Figure S3), and actin binding of the utrophin tandem CH domain and its isolated CH domains (Figure S4) (PDF)

## ■ AUTHOR INFORMATION

### ■ Corresponding Author

\*Address: 12850 E. Montview Blvd., C238, Skaggs School of Pharmacy and Pharmaceutical Sciences, University of Colorado Anschutz Medical Campus, Aurora, CO 80045. E-mail: krishna.

mallela@ucdenver.edu. Phone: 1-303-724-3576. Fax: 1-303-724-7266.

### ■ Author Contributions

S.M.S. and S.B. contributed equally to this work.

### ■ Funding

This project was funded by the American Heart Association, Jane and Charlie Butcher grants in Genomics and Biotechnology, and the ALSAM Foundation through the Skaggs Scholars Program.

### ■ Notes

The authors declare no competing financial interest.

## ■ ACKNOWLEDGMENTS

We sincerely thank Steve Winder for many helpful discussions about CH domains. We appreciate the help from Shyam Mehta and Dinen Shah in performing some of the experiments. We thank David Bain, Carlos Catalano, and Walter Englander for their critical reading of the manuscript.

## ■ ABBREVIATIONS

ABD, actin-binding domain; ABS, actin-binding surface;  $B_{\max}$ , maximal number of binding sites; CD, circular dichroism; CH, calponin-homology; CH1, N-terminal CH; CH2, C-terminal CH;  $\Delta G_{\text{unf}}$ , Gibbs free energy of unfolding; DSC, differential scanning calorimetry; FT-IR, Fourier transform infrared;  $K_d$ , dissociation constant; MALDI-TOF, matrix-assisted laser desorption ionization time-of-flight;  $T_m$ , melting temperature.

## ■ REFERENCES

- (1) Dominguez, R., and Holmes, K. C. (2011) Actin structure and function. *Annu. Rev. Biophys.* 40, 169–186.
- (2) Korenbaum, E., and Rivero, F. (2002) Calponin homology domains at a glance. *J. Cell Sci.* 115, 3543–3545.
- (3) Gimona, M., and Winder, S. J. (2008) The calponin homology (CH) domain. In *Protein Science Encyclopedia* (Fersht, A., Ed.) pp 1–16, Wiley-VCH Verlag GmbH & Co. KGaA, Weinheim, Germany.
- (4) Sjöblom, B., Ylänne, J., and Djinić-Carugo, K. (2008) Novel structural insights into F-actin-binding and novel functions of calponin homology domains. *Curr. Opin. Struct. Biol.* 18, 702–708.
- (5) Aartsma-Rus, A., van Deutekom, J. C. T., Fokkema, I. F., van Ommen, G.-J. B., and Den Dunnen, J. T. (2006) Entries in the Leiden Duchenne muscular dystrophy mutation database: An overview of mutation types and paradoxical cases that confirm the reading-frame rule. *Muscle Nerve* 34, 135–144.
- (6) Blake, D. J., Weir, A., Newey, S. E., and Davies, K. E. (2002) Function and genetics of dystrophin and dystrophin-related proteins in muscle. *Physiol. Rev.* 82, 291–329.
- (7) Ervasti, J. M. (2007) Dystrophin, its interactions with other proteins, and implications for muscular dystrophy. *Biochim. Biophys. Acta, Mol. Basis Dis.* 1772, 108–117.
- (8) Muir, L. A., and Chamberlain, J. S. (2009) Emerging strategies for cell and gene therapy of the muscular dystrophies. *Expert Rev. Mol. Med.* 11, e18.
- (9) Fairclough, R. J., Bareja, A., and Davies, K. E. (2011) Progress in therapy for Duchenne muscular dystrophy. *Exp. Physiol.* 96, 1101–1113.
- (10) Singh, S. M., Kongari, N., Cabello-Villegas, J., and Mallela, K. M. G. (2010) Missense mutations in dystrophin that trigger muscular dystrophy decrease protein stability and lead to cross- $\beta$  aggregates. *Proc. Natl. Acad. Sci. U. S. A.* 107, 15069–15074.
- (11) Henderson, D. M., Lee, A., and Ervasti, J. M. (2010) Disease-causing missense mutations in actin binding domain 1 of dystrophin induce thermodynamic instability and protein aggregation. *Proc. Natl. Acad. Sci. U. S. A.* 107, 9632–9637.



- (12) Deol, J. R., Danialou, G., Larochele, N., Bourget, M., Moon, J. S., Liu, A. B., Gilbert, R., Petrof, B. J., Nalbantoglu, J., and Karpati, G. (2007) Successful compensation for dystrophin deficiency by a helper-dependent adenovirus expressing full-length utrophin. *Mol. Ther.* 15, 1767–1774.
- (13) Henderson, D. M., Belanto, J. J., Li, B., Heun-Johnson, H., and Ervasti, J. M. (2011) Internal deletion compromises the stability of dystrophin. *Hum. Mol. Genet.* 20, 2955–2963.
- (14) Le Rumeur, E., Winder, S. J., and Hubert, J.-F. (2010) Dystrophin: More than just the sum of its parts. *Biochim. Biophys. Acta, Proteins Proteomics* 1804, 1713–1722.
- (15) Winder, S. J., Knight, A. E., and Kendrick-Jones, J. (1997) Protein Structure. In *Dystrophin: Gene, protein and cell biology* (Brown, S. C., and Lucy, J. A., Eds.) pp 27–55, Cambridge University Press, Cambridge, U.K.
- (16) Levine, B. A., Moir, A. J., Patchell, V. B., and Perry, S. V. (1990) The interaction of actin with dystrophin. *FEBS Lett.* 263, 159–162.
- (17) Levine, B. A., Moir, A. J., Patchell, V. B., and Perry, S. V. (1992) Binding sites involved in the interaction of actin with the N-terminal region of dystrophin. *FEBS Lett.* 298, 44–48.
- (18) Norwood, F. L. M., Sutherland-Smith, A. J., Keep, N. H., and Kendrick-Jones, J. (2000) The structure of the N-terminal actin-binding domain of human dystrophin and how mutations in this domain may cause Duchenne or Becker muscular dystrophy. *Structure* 8, 481–491.
- (19) Keep, N. H., Winder, S. J., Moores, C. A., Walke, S., Norwood, F. L., and Kendrick-Jones, J. (1999) Crystal structure of the actin-binding region of utrophin reveals a head-to-tail dimer. *Structure* 7, 1539–1546.
- (20) Winder, S. J., Hemmings, L., Maciver, S. K., Bolton, S. J., Tinsley, J. M., Davies, K. E., Critchley, D. R., and Kendrick-Jones, J. (1995) Utrophin actin binding domain: analysis of actin binding and cellular targeting. *J. Cell Sci.* 108 (Part 1), 63–71.
- (21) Singh, S. M., Bandi, S., Winder, S. J., and Mallela, K. M. G. (2014) The actin binding affinity of the utrophin tandem calponin-homology domain is primarily determined by its N-terminal domain. *Biochemistry* 53, 1801–1809.
- (22) Bandi, S., Singh, S. M., and Mallela, K. M. G. (2014) The C-terminal domain of the utrophin tandem calponin-homology domain appears to be thermodynamically and kinetically more stable than the full-length protein. *Biochemistry* 53, 2209–2211.
- (23) Mossessova, E., and Lima, C. D. (2000) Ulp1-SUMO crystal structure and genetic analysis reveal conserved interactions and a regulatory element essential for cell growth in yeast. *Mol. Cell* 5, 865–876.
- (24) Greenfield, N. J. (2007) Using circular dichroism spectra to estimate protein secondary structure. *Nature Protoc.* 1, 2876–2890.
- (25) Reijenga, J. C., Gagliardi, L. G., and Kenndler, E. (2007) Temperature dependence of acidity constants, a tool to affect separation selectivity in capillary electrophoresis. *J. Chromatogr. A* 1155, 142–145.
- (26) <http://www.tainstruments.com/pdf/literature/MCTN-2011-04%20Buffer%20Compatibility%20with%20Nano%20DSC.pdf>.
- (27) Santoro, M. M., and Bolen, D. W. (1992) A test of the linear extrapolation of unfolding free energy changes over an extended denaturant concentration range. *Biochemistry* 31, 4901–4907.
- (28) Santoro, M. M., and Bolen, D. W. (1988) Unfolding free energy changes determined by the linear extrapolation method. 1. Unfolding of phenylmethanesulfonyl alpha-chymotrypsin using different denaturants. *Biochemistry* 27, 8063–8068.
- (29) Tal, M., Silberstein, A., and Nusser, E. (1985) Why does Coomassie Brilliant Blue R interact differently with different proteins? A partial answer. *J. Biol. Chem.* 260, 9976–9980.
- (30) Singh, S. M., Bandi, S., Shah, D. D., Armstrong, G., and Mallela, K. M. G. (2014) Missense mutation Lys18Asn in dystrophin that triggers X-linked dilated cardiomyopathy decreases protein stability, increases protein unfolding, and perturbs protein structure, but does not affect protein function. *PLoS One* 9, e110439.
- (31) Lakowicz, J. R. (2006) *Principles of Fluorescence Spectroscopy*, 3rd ed., Springer Science, New York.
- (32) Pace, C. N. (1986) Determination and analysis of urea and guanidine hydrochloride denaturation curves. *Methods Enzymol.* 131, 266–280.
- (33) Freire, E. (1995) Thermal denaturation methods in the study of protein folding. *Methods Enzymol.* 259, 144–168.
- (34) Stark, G. R. (1965) Reactions of cyanate with functional groups of proteins. 3. Reactions with amino and carboxyl groups. *Biochemistry* 4, 1030–1036.
- (35) Shaw, W. H. R., and Bordeaux, J. J. (1955) The decomposition of urea in aqueous media. *J. Am. Chem. Soc.* 77, 4729–4733.
- (36) Prakash, V., Loucheux, C., Scheufele, S., Gorbunoff, M. J., and Timasheff, S. N. (1981) Interactions of proteins with solvent components in 8 M urea. *Arch. Biochem. Biophys.* 210, 455–464.
- (37) Lowenthal, M. S., Khanna, R. K., and Moore, M. H. (2002) Infrared spectrum of solid isocyanic acid (HNCO): Vibrational assignments and integrated band intensities. *Spectrochim. Acta, Part A* 58, 73–78.
- (38) Kieke, M. L., Schoppelrei, J. W., and Brill, T. B. (1996) Spectroscopy of hydrothermal reactions. 1. The CO<sub>2</sub>-H<sub>2</sub>O system and kinetics of urea decomposition in an FTIR spectroscopy flow reactor cell operable to 725 K and 335 bar. *J. Phys. Chem.* 100, 7455–7462.
- (39) Batey, S., Nickson, A. A., and Clarke, J. (2008) Studying the folding of multidomain proteins. *HFSP J.* 2, 365–377.
- (40) Way, M., Pope, B., and Weeds, A. G. (1992) Evidence for functional homology in the F-actin binding domains of gelsolin and  $\alpha$ -actinin: Implications for the requirements of severing and capping. *J. Cell Biol.* 119, 835–842.
- (41) Rybakova, I. N., Humston, J. L., Sonnemann, K. J., and Ervasti, J. M. (2006) Dystrophin and utrophin bind actin through distinct modes of contact. *J. Biol. Chem.* 281, 9996–10001.
- (42) Bandi, S., Singh, S. M., and Mallela, K. M. G. (2015) Interdomain linker determines primarily the structural stability of dystrophin and utrophin tandem calponin-homology domains rather than their actin-binding affinity. *Biochemistry* 54, 5480–5488.
- (43) Chakravarty, D., Chakraborti, S., and Chakraborti, P. (2015) Flexibility in the N-terminal actin-binding domain: Clues from in silico mutations and molecular dynamics. *Proteins: Struct., Funct., Genet.* 83, 696–710.
- (44) Arviv, O., and Levy, Y. (2012) Folding of multidomain proteins: Biophysical consequences of tethering even in apparently independent folding. *Proteins: Struct., Funct., Genet.* 80, 2780–2798.
- (45) Lin, A. Y., Prochniewicz, E., James, Z. M., Svensson, B., and Thomas, D. D. (2011) Large-scale opening of utrophin's tandem calponin homology (CH) domains upon actin binding by an induced-fit mechanism. *Proc. Natl. Acad. Sci. U. S. A.* 108, 12729–12733.
- (46) Singh, S. M., and Mallela, K. M. G. (2012) The N-terminal actin-binding tandem calponin-homology (CH) domain of dystrophin is in a closed conformation in solution and when bound to F-actin. *Biophys. J.* 103, 1970–1978.
- (47) Kallenbach, N. R., and Dominguez, R. (2012) Dystrophin's tandem calponin-homology domains: Is the case closed? *Biophys. J.* 103, 1818–1819.
- (48) Singh, S. M., Molas, J. F., Kongari, N., Bandi, S., Armstrong, G. S., Winder, S. J., and Mallela, K. M. G. (2012) Thermodynamic stability, unfolding kinetics, and aggregation of the N-terminal actin-binding domains of utrophin and dystrophin. *Proteins: Struct., Funct., Genet.* 80, 1377–1392.
- (49) Grdadolnik, J., and Maréchal, Y. (2002) Urea and urea-water solutions - an infrared study. *J. Mol. Struct.* 615, 177–189.

## SUPPORTING INFORMATION

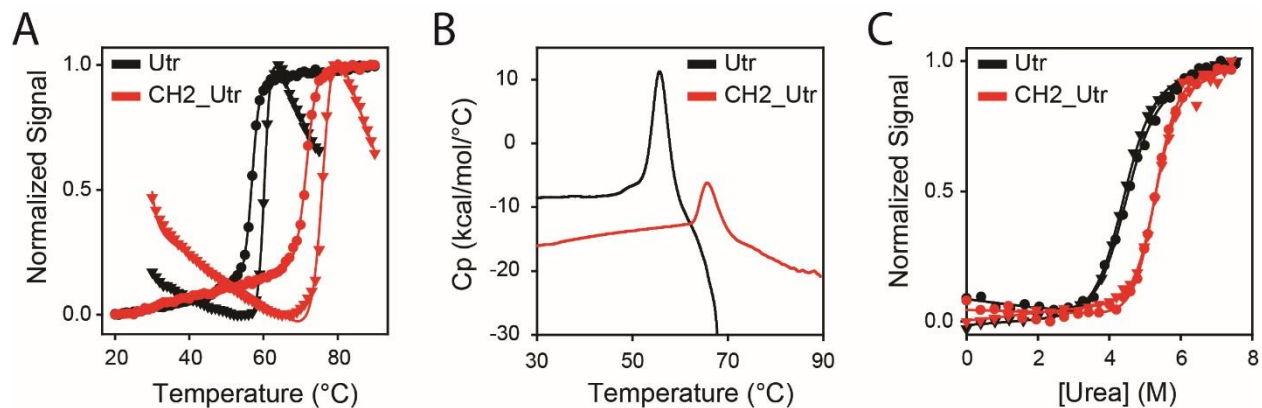


**Figure S1:** Structural stability of utrophin tandem CH domain and its isolated CH2 domain. (A) Changes in the CD signal at 222 nm (circles) and in the intrinsic protein fluorescence (triangles) of the tandem CH domain (black) and its CH2 domain (red) as a function of increasing solution temperature <sup>(22)</sup>. (B) DSC thermograms for the tandem CH domain (black) and its CH2 domain (red). (C) Changes in the CD signal at 222 nm (circles) and in the intrinsic protein fluorescence (triangles) of the tandem CH domain (black) and its CH2 domain (red) as a function of increasing urea concentration <sup>(22)</sup>.

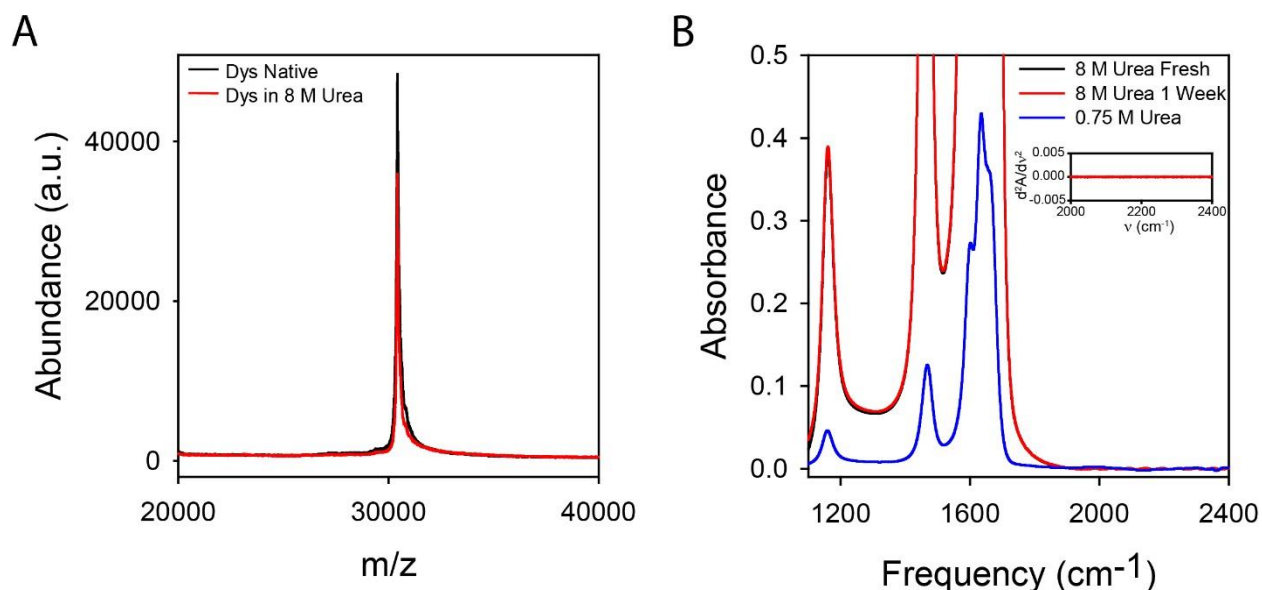


**Figure S2:** (A) MALDI-TOF mass spectrometry of dystrophin tandem CH domain in the absence (black) and in the presence (red) of 8 M urea. Identical mass ( $30,427 \pm 30$  Da) indicates that high urea concentration is not chemically modifying the protein. (B) FT-IR characterization of urea degradation over time. Blue, black, and red curves show the spectra of 0.75 M urea freshly prepared, 8 M urea freshly prepared, and 8 M urea after one week of preparation, respectively. FT-IR spectrum of 0.75 M urea matches with that reported in the literature <sup>(49)</sup>. For 8 M urea samples, the spectra were shown below 0.5 absorbance to indicate that no spectral changes were observed after one week of preparation. In particular, no new peaks were observed around  $2200\text{ cm}^{-1}$ , which is the characteristic frequency region corresponding to cyanate <sup>(37, 38)</sup>, the main degradation product of urea <sup>(32)</sup>. This is also evident from the second derivative spectra of the absorbance shown in the Inset of Figure S2B.

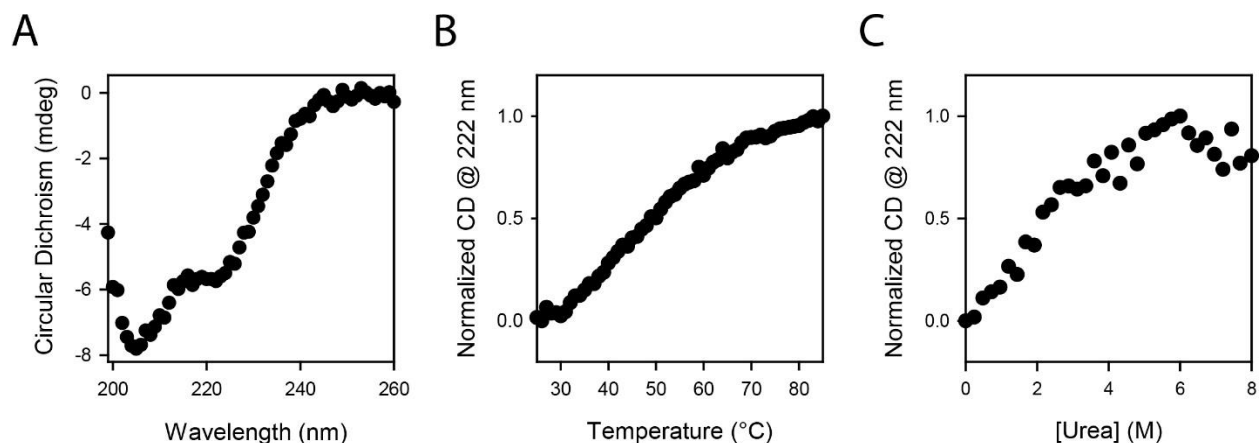


**Figure S3:** Isolated CH1 domain of utrophin is a partially unfolded, molten globule-like structure. (A) Circular dichroism (CD) spectrum shows decreased  $\alpha$ -helical structure (@222 nm) and increased random coil structure (@ 205 nm) compared to the CD spectra of full-length utrophin tandem CH domain or its isolated CH2 domain <sup>(22)</sup>. (B) Thermal melt and (C) denatured melt of CH1 domain show half-sigmoidal transitions with missing native baselines, whereas the corresponding melts of full-length utrophin tandem CH domain and its isolated CH2 domain show complete sigmoidal, cooperative transitions with proper native and unfolded baselines (Figures S1A & S1C). The incomplete sigmoidal transitions for CH1 domain indicate that it is a partially unfolded, molten globule-like structure.

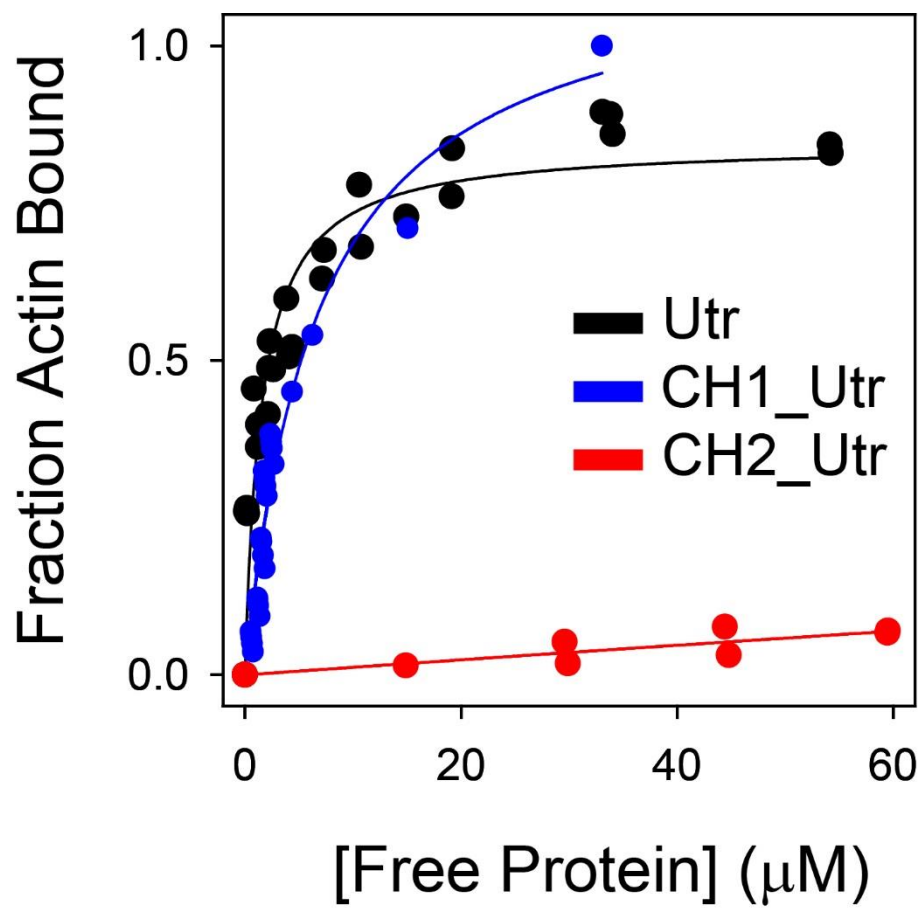


**Figure S4:** Actin binding curves of utrophin tandem CH domain (black), its CH1 (blue) and CH2 (red) domains <sup>(21)</sup>.